Fibers and Polymers 2006, Vol.7, No.1, 42-50

Anisotropic-Asymmetric Yield Criterion and Anisotropic Hardening Law for Composite Materials: Theory and Formulations

Ji Hoon Kim, Myoung-Gyu Lee[1], Kwansoo Chung*, Jae Ryoun Youn, and Tae Jin Kang

School of Materials Science and Engineering, Seoul National University, Seoul 151-744, Korea
[1]Department of Materials Science and Engineering, Ohio State University, USA
(Received October 30, 2005; Revised February 1, 2006; Accepted February 12, 2006)

Abstract: In this paper, elasto-plastic constitutive equations for highly anisotropic and asymmetric materials are developed and their numerical implementation is presented. Some engineering materials such as fiber reinforced composites show different material behavior in the different material directions (anisotropy) as well as in tension and compression (asymmetry). Although these materials have mostly been analyzed using the anisotropic elastic constitutive equations, the necessity of consideration of plastic properties has been frequently reported in the previous works. In order to include both the anisotropic and asymmetric properties of composite materials, the Drucker-Prager yield criterion is modified by adding anisotropic parameters and initial components of translation. The implementation procedure for the developed theory and algorithms is presented based on the implicit finite element scheme. The measured data from the previous work are used to validate the present constitutive equations.

Keywords: Constitutive equations, Drucker-Prager yield criterion, Anisotropy, Asymmetry, Fiber reinforced composites

Introduction

Many engineering materials have anisotropy which shows different material behavior with respect to different directions. Fiber reinforced materials, which show strong anisotropy [1], also show deviatory mechanical behavior under tensile and compressive loading conditions. The difference of elastic properties in tension and compression has generally been called asymmetry or bi-modular [2-4] property. Fiber reinforced composite materials have frequently been considered to be elastically anisotropic and most of mechanical analysis have been performed using linear elastic constitutive equations. However, more sophisticated description requires consideration of some forms of plasticity, viscoelasticity, or both. Recently experimental studies under static loading revealed that fiber reinforced composites showed nonlinear behavior for which the constitutive equations were investigated by elasto-plasticity [5] and by elastic damage theory [6]. In this paper, the constitutive equations to describe the material behavior of composite materials are presented. To include the anisotropy as well as asymmetric properties of composites materials, the conventional yield criterion for metallic and/or porous materials is modified and a numerical algorithm for the finite element method is presented.

The yielding of porous materials such as concrete and soil can be effectively described by adding the pressure sensitive terms to the isotropic yield functions which are generally used for metallic materials. The Coulomb-Mohr criterion and Drucker-Prager criterion are the most well known ones for the purpose. Since the two yield criteria include the influence of the hydrostatic pressure, the shapes of the yield surfaces are conical and they show different yield stress in tension and compression. Therefore, these yield surfaces can be used for asymmetric materials with the plane stress assumption without complicated modifications. However, the Coulomb-Mohr criterion has corner shape like Tresca yield surface, which makes difficulty in applying the classical associated plasticity theory to determine unique plastic strain increment. On the other hand, Drucker and Prager suggested smooth circular cone-shaped yield surface by adding hydrostatic term to the isotropic von Mises yield surface [7]. Therefore, the Drucker-Prager yield surface has been chosen as the base yield criterion to be modified.

For the anisotropy of composites materials, Hill modified and extended the isotropic Mises yield function [8]. He assumed that material has three mutually orthogonal planes of symmetry at each material point and the hydrostatic stress does not affect yielding. Recently Barlat *et al.* [9,10] proposed anisotropic yield functions especially for the aluminum alloys. They used a linear transformation of the Cauchy stress to consider isotropic function. In order to consider both the anisotropy and asymmetry, the anisotropic yield function should be modified. One way to achieve this is to introduce the pressure dependent terms which make the yield surface show different initial yield stress in tension and compression.

As for the hardening behavior, previous efforts to implement plasticity considered mainly three types of hardening assumptions. Isotropic hardening assumes that the yield surface can expand only without translation, while kinematic hardening translates without size change. The combined isotropic-kinematic hardening allows both the expansion and translation of yield surface. Leewood *et al.* [11] used the isotropic hardening to describe plastic properties of fibrous metal composites. Isupov *et al.* [12] dealt with the micromechanical analysis of plastic deformation processes of metal matrix composites composed of elastic reinforcing elements and the plastic

*Corresponding author: kchung@snu.ac.kr

matrix based on the generalized anisotropic Prager type kinematic hardening law. Recently, Sarbayev [13] described the plasticity theory for anisotropic composites utilizing the kinematic hardening of the anisotropic quadratic yield surface. Lee *et al.* [14] discussed the necessity of anisotropic evolution rule which can explain the directionality of back-stress evolution. In this paper, a kinematic hardening law is introduced to describe anisotropic hardening behavior of highly anisotropic materials such as fiber reinforced composites by modifying the nonlinear back-stress evolution rule by Chaboche [15].

This paper focuses on the numerical algorithms, especially on the stress integration procedure for the finite element method. The developed constitutive equations do not restrict the choice of hardening laws so that the theory and algorithms can be applied to the general combined nonlinear isotropic-kinematic hardening rules.

Constitutive Equations

Anisotropic Elasticity

The stress-strain relationship for the anisotropic materials is generally derived from the generalized Hooke's law.

$$\boldsymbol{\sigma} = \mathbf{C}\boldsymbol{\varepsilon}^e \tag{1}$$

where $\boldsymbol{\sigma}$ is the Cauchy stress tensor, $\mathbf{C}$ is the stiffness matrix, and $\boldsymbol{\varepsilon}^e$ is the elastic strain tensor. For 3-dimensional anisotropic materials, 21 independent material constants are needed to describe material behavior but only 4 independent material constants are enough under the assumption of orthotropic and plane stress condition. The stress-strain relation of an orthotropic material under the plane stress condition can be described as following:

$$\begin{Bmatrix} \sigma_x \\ \sigma_y \\ \sigma_{xy} \end{Bmatrix} = \begin{bmatrix} Q_{11} & Q_{12} & 0 \\ Q_{12} & Q_{22} & 0 \\ 0 & 0 & Q_{66} \end{bmatrix} \begin{Bmatrix} \varepsilon_x \\ \varepsilon_y \\ \varepsilon_{xy} \end{Bmatrix} \tag{2}$$

The reduced stiffness Q_{ij} above are expressed in terms of engineering constants,

$$Q_{11} = \frac{E_x}{1 - \nu_{xy}\nu_{yx}}$$

$$Q_{12} = \frac{\nu_{xy}E_y}{1 - \nu_{xy}\nu_{yx}} = \frac{\nu_{yx}E_x}{1 - \nu_{xy}\nu_{yx}}$$

$$Q_{22} = \frac{E_y}{1 - \nu_{xy}\nu_{yx}}$$

$$Q_{66} = G_{xy} \tag{3}$$

where E_x, E_y and ν_{xy}, ν_{yx} are Young's moduli and Poisson's ratios for the two material directions shown in Figure 1, G_{xy} is in-plane shear modulus. Note that the two Poisson's ratios are not independent and have the following reciprocal relation [16].

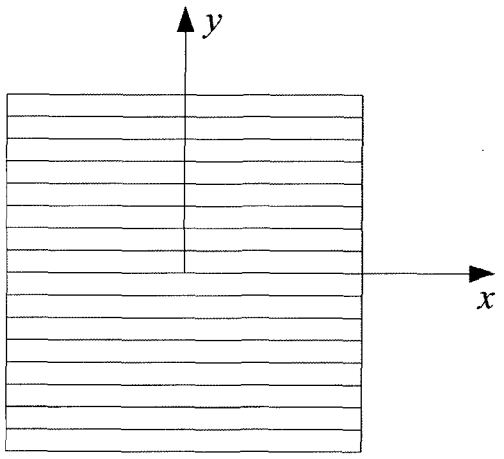

Figure 1. Material directions for orthotropic materials under plane stress condition.

$$\frac{\nu_{xy}}{E_x} = \frac{\nu_{yx}}{E_y} \tag{4}$$

As explained in the introduction of this paper, fiber reinforced composite materials have bi-modular property (or asymmetric property) showing different tensile and compressive properties. In order to predict the bi-modular property the elastic constants in equation (2) should be measured both in the tensile and compressive directions. Here, the superscripts 'T' and 'C' represent tensile and compressive properties, respectively. For example, E_x^T and E_x^C mean the tensile and compressive moduli in the x direction illustrated in Figure 1.

Plasticity Theory Based on Metal Plasticity

Although the composite materials have been generally considered as anisotropic elastic material, recent experiments confirm that fiber reinforced composites show plastic behavior in addition to elastic behavior. For a long time, plasticity theory has been developed to represent the nonlinearity of stress-strain relationship. For this purpose, the yield surface has been mathematically imagined to divide the stress space into the elastic and plastic regions. If a stress state at a point satisfies the yield criterion, then this point deforms plastically, otherwise it undergoes elastic deformation. Traditionally, most of yield surfaces have been developed for metallic materials. The most well-known yield criteria are von Mises and Tresca yield criteria. These yield surfaces, however, can only describe isotropic property which has no directional difference of initial yielding.

In order to include the yield behavior of anisotropic materials, many anisotropic yield surfaces have been developed by modifying the isotropic yield surface such as von Mises and Tresca yield surfaces. One of the well-known anisotropic yield surfaces is Hill's orthotropic yield criterion which modified von Mises yield surface by introducing additional material

parameters showing directional differences of initial yield stresses [8]. Under the plane stress assumption, it has the form of

$$\Phi = f(\boldsymbol{\sigma}) - \bar{\sigma}_{iso}^2 = \boldsymbol{\sigma}^T \boldsymbol{B} \boldsymbol{\sigma} - \bar{\sigma}_{iso}^2 = 0 \quad (5)$$

where $\boldsymbol{B} = \begin{bmatrix} b_{11} & b_{12} & 0 \\ b_{12} & b_{22} & 0 \\ 0 & 0 & b_{66} \end{bmatrix}$ and $\bar{\sigma}_{iso}$ is the equivalent stress measuring the size of the yield surface as the first order homogeneous function. The material constants in **B** matrix characterize the anisotropic yield behavior and can be measured by performing uni-axial tension tests in two principal directions of anisotropy and one pure shear test on the orthogonal plane of anisotropy.

In addition to yield surface, hardening law is needed to describe the evolution of yield surface. In general, three types of hardening assumptions have been suggested for the most engineering materials including metals and composites: either yield surface can only expand monotonically and the amount of hardening depends on the effective plastic strain (isotropic hardening) or yield surface can only translates in the stress space and the amount of translation also depends on the effective plastic strain (kinematic hardening), which satisfies the general plastic work equivalence principle [17] for monotonously proportional loading. Another hardening rule which describes the expansion and translation of the yield surface has been developed recently (isotropic-kinematic hardening) to predict both the transient and Bauschinger effect [7]. In Figure 2, schematic view of the three types of hardening laws is illustrated.

For the back stress increment of kinematic hardening, the Chaboche model has been used to consider non-linear behavior of stress-strain curves. The hardening rule of Chaboche type back stress evolution rule is,

$$d\boldsymbol{\alpha} = d\boldsymbol{\alpha}_1 - d\boldsymbol{\alpha}_2 \quad (6)$$

$$d\boldsymbol{\alpha}_1 = c \cdot \frac{(\boldsymbol{\sigma} - \boldsymbol{\alpha})}{\bar{\sigma}_{iso}} d\bar{\varepsilon}, \quad d\boldsymbol{\alpha}_2 = h d\bar{\varepsilon} \boldsymbol{\alpha} \quad (7)$$

where c and h are material constants to be determined experimentally [15].

Although above hardening laws can be used with the anisotropic yield surfaces, the new hardening law incorporating directional difference is essential to properly describe the constitutive behavior of highly anisotropic materials. In addition to the hardening law, the new yield surface should be considered because plastic behavior also has the asymmetric property. In the following section, the new yield surface and hardening rule which can describe both the anisotropy and asymmetry are explained in detail.

Plasticity for Composite Materials

Since fiber reinforced composites are reinforced by either short or long fibrous materials, they have two unique properties compared with metallic materials: highly unequal strength in different material directions (anisotropy) and unequal strength in tension and compression (bi-modular or asymmetry). The conventional anisotropic yield surface can describe the initial highly anisotropic yield strength but the directional difference of evolution of yield surface cannot be effectively explained with the general hardening rules which satisfy the equivalent plastic work principle. Also, the asymmetric properties cannot be achieved with the yield surface commonly used in metal plasticity. Here, in order to consider these two unique characteristics of composite materials, the Drucker-Prager yield surface was modified by incorporating anisotropic parameters under the plane stress assumption. As for the hardening rule, new anisotropic hardening evolution rule with directionality is developed. In addition to the theoretical development of constitutive equations, the numerical implementation procedure is also presented in the section.

Anisotropic-Asymmetric Constitutive Model

Tsai and Wu [18] introduced a failure criterion in a general quadratic form:

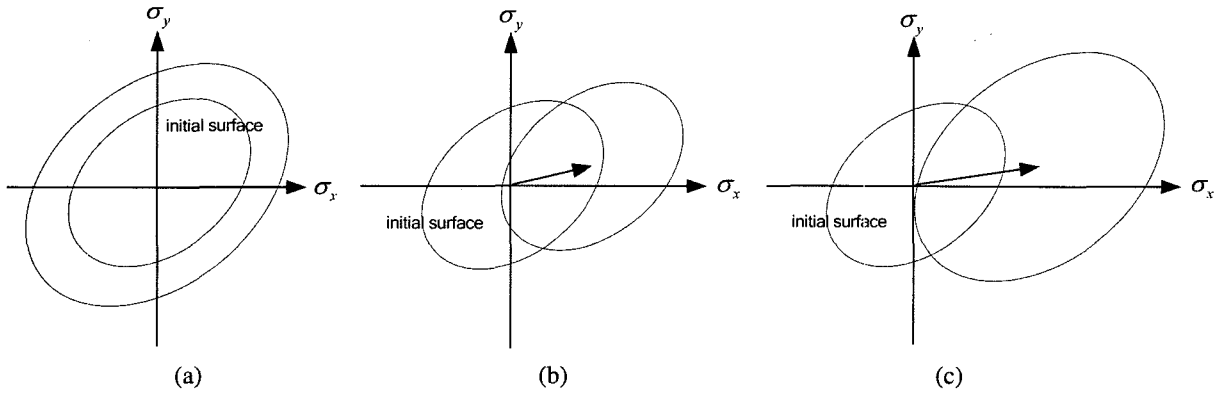

Figure 2. Schamatic view of three types of hardening laws: (a) isotropic hardening, (b) kinematic hardening, (c) isotropic-kinematic hardening.

$$F_i\sigma_i + F_{ij}\sigma_i\sigma_j = 0, \quad i,j = 1,2,\ldots,6 \tag{8}$$

where F_i and F_{ij} are material parameters. For isotropic materials, the Drucker-Prager yield function is obtained from Eq. (8):

$$\Phi = J_2'^{1/2} - qJ_1 - \bar{\sigma}_{iso} = 0 \tag{9}$$

where $J_2' = 1/2S_{ij}S_{ij}$ and $J_1 = \sigma_{kk}$. Here the second order tensor **S** is the deviatoric stress tensor and the above equation reduces to the Mises yield surface when material constant q is zero. To include the orthotropic properties of composite materials, the anisotropic material constants are included in equation (9) after considering the plane stress condition. Then, equation (9) can be modified as,

$$\Phi' = p(\sigma_x^2 - \beta_{22}\sigma_x\sigma_y + \beta_{22}^2\sigma_y^2 + 3\beta_{33}^2\sigma_{xy}^2)^{1/2} - q(\sigma_x + \beta_{22}\sigma_y) - \bar{\sigma}_{iso} = 0 \tag{10}$$

where p, q, β_{22} and β_{33} are material constants characterizing the anisotropic and asymmetric behavior. However, one more material constant is required to represent full orthotropy and asymmetry because the ratios of initial yield stress in two directions are same for tensile and compressive loading cases (incomplete orthotropic Drucker-Prager type). There may be many different ways to achieve fully orthotropic as well as asymmetry. Here, the above orthotropic yield criterion is translated initially to add one more material constant, which can be explained as having initial back-stress.

$$\Phi'' = p[(\sigma_x-\alpha_x)^2 - \beta_{22}(\sigma_x-\alpha_x)(\sigma_y-\alpha_y) + \beta_{22}^2(\sigma_y-\alpha_y)^2 + 3\beta_{33}^2(\sigma_{xy}-\alpha_{xy})^2]^{1/2} - q((\sigma_x-\alpha_x) + \beta_{22}(\sigma_y-\alpha_y)) - \bar{\sigma}_{iso} = 0 \tag{11}$$

where α is the back stress. Because we need only one additional material constant to represent different initial yield stresses for tension and compression in each material direction, the yield surface is translated in one material direction for simplicity. Here, the yield surface is assumed to be initially translated in the y direction. That is, $\alpha_x = \alpha_{xy} = 0$ and $\alpha_y = \alpha_0$ initially. By adding one more parameter the yield surface can describe complete orthotropic Drucker-Prager type yield surface.

To determine the five material constants, it is necessary to measure two uni-axial tensile yield stresses σ_x^T, σ_y^T two compressive yield stresses σ_x^C, σ_y^C and one shear yield stress σ_{xy}^Y. By the measured initial yield stresses and equation (11), the following five non-linear systems of equations are obtained.

$$p\sqrt{(\beta_{22}\alpha_0)^2 + \sigma_x^T\beta_{22}\alpha_0 + (\sigma_x^T)^2} - q(\sigma_x^T - \beta_{22}\alpha_0) - \sigma_x^T = 0 \tag{12-1}$$

$$p\sqrt{(\beta_{22}\alpha_0)^2 - \sigma_x^C\beta_{22}\alpha_0 + (\sigma_x^C)^2} + q(\sigma_x^C + \beta_{22}\alpha_0) - \sigma_x^T = 0 \tag{12-2}$$

$$p\left|\beta_{22}(\sigma_y^T - \alpha_0)\right| - q\beta_{22}(\sigma_y^T - \alpha_0) - \sigma_x^T = 0 \tag{12-3}$$

$$p\left|\beta_{22}(\sigma_y^C + \alpha_0)\right| + q\beta_{22}(\sigma_y^C + \alpha_0) - \sigma_x^T = 0 \tag{12-4}$$

$$p\sqrt{\beta_{22}^2\alpha_0^2 + 3\beta_{33}^2(\sigma_{xy}^Y)^2} + q\beta_{22}\alpha_0 - \sigma_x^T = 0 \tag{12-5}$$

Note that the reference state of stress is uni-axial tensile yield stress in the x direction and the above five equations can be solved by Newton-Raphson method. The two yield surfaces explained above are schematically drawn in Figure 3 for comparison.

Note: Alternate Approach for the Yield Surface

As mentioned before, the yield surface for anisotropic-

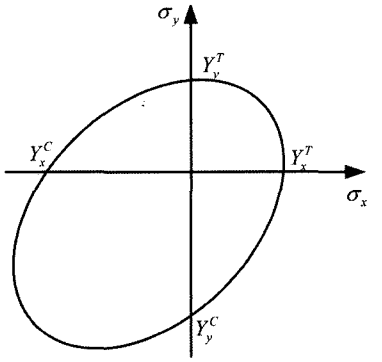

$Y_x^T = Y_y^T \neq Y_x^C = Y_y^C$

(a)

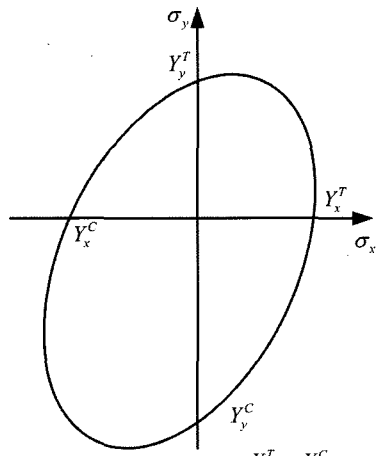

$Y_x^T \neq Y_y^T \neq Y_x^C \neq Y_y^C$ and $\frac{Y_y^T}{Y_x^T} \neq \frac{Y_y^C}{Y_x^C}$

(b)

Figure 3. Schematic view of two types of yield surfaces: (a) Drucker-Prager type and (b) orthotropic asymmetric type.

asymmetric materials can have other alternative ways. Here, for illustrational purpose, the Drucker-Prager type yield surface is tilted by introducing weighting parameter in the pressure term. The yield surface can be written as

$$\Psi = p'[\sigma_x^2 + \beta_{22}'^2\sigma_y^2 - \beta_{22}'\sigma_x\sigma_y + 3\beta_{33}'\sigma_{xy}^2]^{1/2} + q'(\sigma_x + \kappa\sigma_y) - \bar{\sigma}_{iso} = 0 \quad (13)$$

where p', q', β_{22}', β_{33}' and κ are material constants characterizing the anisotropic and asymmetric behavior. In above equation, κ has different value from β_{22}' which makes the orthogonal yield surface tilted with respect to axis of yield surface. Then the material constants have the following relationships with yield stresses:

$$p' = \frac{1}{2}\left(1 + \frac{\sigma_x^T}{\sigma_x^C}\right) \quad (14\text{-}1)$$

$$q' = \frac{1}{2}\left(1 - \frac{\sigma_x^T}{\sigma_x^C}\right) \quad (14\text{-}2)$$

$$\beta_{22}' = \left(\frac{1}{\sigma_y^T} + \frac{1}{\sigma_y^C}\right)\Big/\left(\frac{1}{\sigma_x^T} + \frac{1}{\sigma_x^C}\right) \quad (14\text{-}3)$$

$$\beta_{33}' = \frac{2}{\sqrt{3}}\left(\frac{1}{\sigma_{xy}^Y}\right)\Big/\left(\frac{1}{\sigma_x^T} + \frac{1}{\sigma_x^C}\right) \quad (14\text{-}4)$$

$$\kappa = \left(\frac{1}{\sigma_y^T} - \frac{1}{\sigma_y^C}\right)\Big/\left(\frac{1}{\sigma_x^T} - \frac{1}{\sigma_x^C}\right) \quad (14\text{-}5)$$

Of the two yield surfaces discussed above, the first one is chosen to describe the following numerical algorithm and implementation.

As for the flow rule and loading/unloading conditions, the associative normality rule has been generally applied in the plasticity field for in-plane components. The plastic strain increment is

$$d\boldsymbol{\varepsilon}^p = d\gamma\frac{\partial\bar{\sigma}(\boldsymbol{\sigma}-\boldsymbol{\alpha})}{\partial(\boldsymbol{\sigma}-\boldsymbol{\alpha})} \quad (15)$$

where $d\gamma$ is proportional positive scalar factor. From the principle of plastic equivalent work with the first order homogenous nature of equation (11), the increment of equivalent plastic strain rate becomes

$$d\bar{\varepsilon} = \frac{(\boldsymbol{\sigma}-\boldsymbol{\alpha})\cdot d\boldsymbol{\varepsilon}^p}{\bar{\sigma}(\boldsymbol{\sigma}-\boldsymbol{\alpha})} = \frac{d\gamma(\boldsymbol{\sigma}-\boldsymbol{\alpha})\cdot\frac{\partial\bar{\sigma}(\boldsymbol{\sigma}-\boldsymbol{\alpha})}{\partial(\boldsymbol{\sigma}-\boldsymbol{\alpha})}}{\bar{\sigma}(\boldsymbol{\sigma}-\boldsymbol{\alpha})} = d\gamma \quad (16)$$

where $\boldsymbol{\alpha}$ and $d\bar{\varepsilon}$ are the back-stress tensor and effective plastic strain increment, respectively. Equation (16) is useful when the effective stress does not have its conjugate strain explicitly defined with respect to the plastic strain increment [19]. The out-of-plane plastic strain increment $d\varepsilon_z^p$ is given from the incompressibility condition, $d\varepsilon_z^p = -d\varepsilon_x^p - d\varepsilon_y^p$.

In this paper, the combination of the isotropic hardening and kinematic hardening models is considered so that the initial yield stress translates and expands simultaneously with plastic deformation. The yield surface of equation (11) is described,

$$\Phi''(\boldsymbol{\sigma}-\boldsymbol{\alpha}, \bar{\sigma}_{iso}) = 0 \quad (17)$$

Note that the back-stress has initial value which is the center of initial yield surface.

In the usual way of describing isotropic-kinematic hardening laws, the effective quantities are defined considering the following modified plastic work equivalence principle. i.e.,

$$dw_{iso} = (\boldsymbol{\sigma}-\boldsymbol{\alpha})\cdot d\boldsymbol{\varepsilon}^p = \bar{\sigma}_{iso}d\bar{\varepsilon} \quad (18)$$

For the back stress increment, the Chaboche model explained in the previous section is used. However, in order to account for the directional difference of the back-stress evolution for the highly anisotropic materials, the anisotropic back-stress evolution law has been proposed by modifying the isotropic evolution rule in equation (7). The back stress evolution rule considered here is:

$$d\boldsymbol{\alpha}_1 = \Gamma_1\cdot\frac{(\boldsymbol{\sigma}-\boldsymbol{\alpha})}{\bar{\sigma}_{iso}}d\bar{\varepsilon} = \Gamma_1\cdot\mathbf{n}d\bar{\varepsilon}$$
$$d\boldsymbol{\alpha}_2 = \Gamma_2\cdot\boldsymbol{\alpha}d\bar{\varepsilon} \quad (19)$$

where Γ_1 and Γ_2 are reduced matrices containing material parameters to be experimentally determined for back-stress evolutions in stead of constants. For the plane stress condition of orthotropic materials, the evolution rule becomes,

$$\begin{bmatrix} d\alpha_x \\ d\alpha_y \\ d\alpha_{xy} \end{bmatrix} = \begin{bmatrix} g_{11} & 0 & 0 \\ 0 & g_{22} & 0 \\ 0 & 0 & g_{33} \end{bmatrix}\begin{bmatrix} n_x \\ n_y \\ n_{xy} \end{bmatrix}d\bar{\varepsilon} - \begin{bmatrix} h_{11} & 0 & 0 \\ 0 & h_{22} & 0 \\ 0 & 0 & h_{33} \end{bmatrix}\begin{bmatrix} \alpha_x \\ \alpha_y \\ \alpha_{xy} \end{bmatrix}d\bar{\varepsilon} \quad (20)$$

where g_{ij} and h_{ij} are components of the Γ_1 and Γ_2 respectively and off-diagonal terms in the matrices are ignored for simplicity. In the material characterization step, the above constants can be obtained by simple tension tests in two directions and one shear test. If the material constants in equation (20) are assumed to be constants the following relationships are obtained for monotonously proportional experiments and the material parameters can be obtained

from the curve fitting of loading curves. Note again that the initial translation α_0 in the y direction is considered here.

$$\begin{bmatrix}\alpha_x\\ \alpha_y\\ \alpha_{xy}\end{bmatrix} = \begin{bmatrix}0\\ \alpha_0\\ 0\end{bmatrix} + \begin{bmatrix}\frac{g_{11}n_x}{h_{11}}(1-e^{-h_{11}\bar{\varepsilon}})\\ \frac{g_{22}n_y}{h_{22}}(1-e^{-h_{22}\bar{\varepsilon}})\\ \frac{g_{33}n_{xy}}{h_{33}}(1-e^{-h_{33}\bar{\varepsilon}})\end{bmatrix} \tag{21}$$

Numerical Implementation of the Constitutive Model

The numerical scheme to solve nonlinear boundary value problems using a finite element method is to iteratively try out discrete displacement increment at the discretized material space and process time until the trial values ultimately satisfy either the static or dynamic principle of momentum at every material element. At the first step, the discrete strain increments are calculated from trial displacement increments and then at the second step, the stresses and other state variables such as plastic strains, back stresses are updated from the discrete strain increments using the elasto-plastic constitutive equations. Finally, the tolerance is checked whether the static or dynamic principle of momentum is satisfied.

For a given strain increment $\Delta\boldsymbol{\varepsilon}$, the numerical formulation provides $\Delta\boldsymbol{\varepsilon}^e$, $\Delta\boldsymbol{\varepsilon}^p$ and $\Delta\boldsymbol{\sigma}$, $\Delta\boldsymbol{\alpha}$, which are

$$\Delta\boldsymbol{\varepsilon}^p = \Delta\gamma\frac{\partial\bar{\sigma}}{\partial(\boldsymbol{\sigma}-\boldsymbol{\alpha})} \tag{22}$$

$$\Delta\boldsymbol{\varepsilon}^e = \Delta\boldsymbol{\varepsilon} - \Delta\boldsymbol{\varepsilon}^p \tag{23}$$

$$\Delta\boldsymbol{\sigma} = \mathbf{C}\cdot\Delta\boldsymbol{\varepsilon}^e = \mathbf{C}\cdot(\Delta\boldsymbol{\varepsilon} - \Delta\boldsymbol{\varepsilon}^p) \tag{24}$$

$$\Delta\boldsymbol{\sigma} = \left(\Gamma_1\cdot\frac{(\boldsymbol{\sigma}-\boldsymbol{\alpha})}{\bar{\sigma}_{iso}} - \Gamma_2\cdot\boldsymbol{\alpha}\right)\Delta\bar{\varepsilon} \tag{25}$$

Note here that all these increments are functions of unknown quantity $\Delta\bar{\varepsilon}$ when the hardening curve is provided. The unknown $\Delta\bar{\varepsilon}$ can be obtained from the following consistency requirement.

$$\Phi''(\boldsymbol{\sigma}_0 - \boldsymbol{\alpha}_0 + \Delta\boldsymbol{\sigma} - \Delta\boldsymbol{\alpha},\ \bar{\varepsilon}_0 + \Delta\bar{\varepsilon}) = 0 \tag{26}$$

where the subscript "0" represents the (initial) values of the previous step.

Based on the constitutive equations developed here, the stress update scheme is outlined using the predictor-corrector method based on the Newton-Raphson method. The updated stress is initially assumed to be elastic for a given discrete strain increment $\Delta\boldsymbol{\varepsilon}$. Therefore,

$$\boldsymbol{\sigma}^T_{n+1} = \boldsymbol{\sigma}_n + \mathbf{C}\Delta\boldsymbol{\varepsilon} \tag{27}$$

where the superscript 'T' stands for a trial state and the subscript denotes the process time step. Also, the trial plastic quantities are preserved as the previous values,

$$\bar{\varepsilon}^T_{n+1} = \bar{\varepsilon}_n \text{ and } \boldsymbol{\alpha}^T_{n+1} = \boldsymbol{\alpha}_n \tag{28}$$

If the following yield condition is satisfied with the trial values for a prescribed elastic tolerance Tol^e for each active surface,

$$\Phi'' = \bar{\sigma}(\boldsymbol{\sigma}^T_{n+1} - \boldsymbol{\alpha}^T_{n+1}) - \bar{\sigma}_{iso}(\bar{\varepsilon}^T_{n+1}) < \text{Tol}^e \tag{29}$$

the process at the step $n+1$ is considered elastic.

If the above condition on yielding is violated ($\Phi > \text{Tol}^e$), the step is considered elasto-plastic and the trial elastic stress state is taken as an initial value for the solution of the plastic corrector problem until the yield condition is satisfied during the iteration. The predictor-corrector scheme based on the Newton-Raphson method was used to solve $\Delta\bar{\varepsilon}$.

Then the nonlinear consistency equations are

$$\Phi = \bar{\sigma}(\boldsymbol{\sigma}-\boldsymbol{\alpha}) - \bar{\sigma}_{iso} = 0 \tag{30}$$

where

$$\boldsymbol{\sigma}_{n+1} = \boldsymbol{\sigma}^T_{n+1} - \mathbf{C}\cdot\Delta\gamma\frac{\partial\bar{\sigma}}{\partial(\boldsymbol{\sigma}_{n+\beta}-\boldsymbol{\alpha}_{n+\beta})} \tag{31}$$

and

$$\boldsymbol{\sigma}_{n+1} = \boldsymbol{\alpha}_n + \left(\Gamma_1\cdot\frac{(\boldsymbol{\sigma}-\boldsymbol{\alpha}_{n+\beta})}{\bar{\sigma}_{iso}} - \Gamma_2\cdot\boldsymbol{\alpha}_{n+\beta}\right)\Delta\bar{\varepsilon} \tag{32}$$

where $0 \le \beta \le 1$. From the linearized form of equation (30),

$$(\delta\Delta\gamma)_{m+1} = -\frac{\Phi_m}{(\partial\Phi/\partial\Delta\gamma)_m} \tag{33}$$

for the m-th iteration and

$$\frac{\partial\Phi}{\partial\Delta\gamma} = \frac{\partial\Phi}{\partial\boldsymbol{\sigma}}\frac{\partial\boldsymbol{\sigma}}{\partial\Delta\gamma} + \frac{\partial\Phi}{\partial\boldsymbol{\alpha}}\frac{\partial\boldsymbol{\alpha}}{\partial\Delta\gamma} + \frac{\partial\Phi}{\partial\bar{\sigma}_{iso}}\frac{\partial\bar{\sigma}_{iso}}{\partial\Delta\gamma} \tag{34}$$

where

$$\frac{\partial\boldsymbol{\sigma}_{n+1}}{\partial\Delta\gamma} = -\mathbf{C}\cdot\frac{\partial\bar{\sigma}}{\partial(\boldsymbol{\sigma}_{n+\beta}-\boldsymbol{\alpha}_{n+\beta})} \tag{35}$$

$$\frac{\partial\boldsymbol{\alpha}_{n+1}}{\partial\Delta\gamma} = \Gamma_1\cdot\frac{(\boldsymbol{\sigma}_{n+\beta}-\boldsymbol{\alpha}_{n+\beta})}{\bar{\sigma}_{iso}} - \Gamma_2\boldsymbol{\alpha}_{n+\beta} \tag{36}$$

while

$$\frac{\partial\Phi}{\partial\boldsymbol{\sigma}_{n+1}} = -\frac{\partial\Phi}{\partial\boldsymbol{\alpha}_{n+1}} = \frac{\partial\bar{\sigma}}{\partial(\boldsymbol{\sigma}_{n+1}-\boldsymbol{\alpha}_{n+1})},\ \text{and}\ \frac{\partial\Phi}{\partial\bar{\sigma}_{iso}} = -1 \tag{37}$$

Note that in deriving equation (36), the higher order terms caused by the variation of stresses with respect to the variation of the effective strain increment have been ignored for simplicity. In order to complete the above equations, the normal of yield surface is needed and

summarized in Appendix.

After obtaining consistency parameters from the above procedures, the stress and other plastic state variables can be updated.

$$\Delta\bar{\varepsilon}_{n+1}^{(m+1)} = \Delta\bar{\varepsilon}_{n+1}^{(m)} + \delta(\Delta\bar{\varepsilon}) \tag{38-1}$$

$$\boldsymbol{\sigma}_{n+1}^{(m+1)} = \boldsymbol{\sigma}_{n+1}^{(m)} + \Delta\boldsymbol{\sigma}_{n+1}(\Delta\bar{\varepsilon}_{n+1}^{(m+1)}) \tag{38-2}$$

$$\boldsymbol{\alpha}_{n+1}^{(m+1)} = \boldsymbol{\alpha}_{n+1}^{(m)} + \Delta\boldsymbol{\alpha}_{n+1}(\Delta\bar{\varepsilon}_{n+1}^{(m+1)}) \tag{38-3}$$

In order to implement the constitutive model into implicit finite element codes, tangent modulus consistent with the integration algorithm developed above is needed to preserve the quadratic rate of convergence that characterizes Newton's method [19,20]. In order to calculate algorithmic tangent modulus, the following consistency equation is considered.

$$\Phi(\boldsymbol{\sigma}_{n+1},\boldsymbol{\alpha}_{n+1}) = \bar{\sigma}(\boldsymbol{\sigma}_{n+1}-\boldsymbol{\alpha}_{n+1}) - \bar{\sigma}_{iso}\bar{\varepsilon}_{n+1} = 0 \tag{39}$$

where

$$\boldsymbol{\sigma}_{n+1} = \boldsymbol{\sigma}_n + \mathbf{C}\cdot[\boldsymbol{\varepsilon}_{n+1}-\boldsymbol{\varepsilon}_n - d\bar{\varepsilon}\mathbf{m}_{n+\beta}] \text{ and}$$

$$\mathbf{m}_{n+\beta} = \frac{\partial\bar{\sigma}}{\partial(\boldsymbol{\sigma}_{n+1}-\boldsymbol{\alpha}_{n+1})} \tag{40}$$

$$\boldsymbol{\alpha}_{n+1} = \boldsymbol{\alpha}_n + \Gamma_1\frac{(\boldsymbol{\sigma}_{n+1}-\boldsymbol{\alpha}_{n+1})}{\bar{\sigma}_{iso}}d\bar{\varepsilon} - \Gamma_2\boldsymbol{\alpha}_{n+1}d\bar{\varepsilon} \tag{41}$$

Note that the approximation is applied to equation (41) for simplicity. Differentiating the above two equations,

$$d\boldsymbol{\sigma}_{n+1} = \bar{\mathbf{C}}\cdot[d\boldsymbol{\varepsilon}_{n+1} - d^2\bar{\varepsilon}\mathbf{m}_{n+\beta} + d\bar{\varepsilon}(\mathbf{M}_{n+\beta}\cdot\boldsymbol{\Omega})d^2\bar{\varepsilon}] \tag{42}$$

where

$$\mathbf{M}_{n+\beta} = \frac{\partial^2\bar{\sigma}}{\partial(\boldsymbol{\sigma}_{n+1}-\boldsymbol{\alpha}_{n+1})\partial(\boldsymbol{\sigma}_{n+1}-\boldsymbol{\alpha}_{n+1})}$$

$$\bar{\mathbf{C}} = [\mathbf{C}^{-1} + d\bar{\varepsilon}\mathbf{M}_{n+\beta}]^{-1} \tag{43}$$

and

$$d\boldsymbol{\alpha}_{n+1} = \left(\Gamma_1\cdot\frac{(\boldsymbol{\sigma}_{n+1}-\boldsymbol{\alpha}_{n+1})}{\bar{\sigma}_{iso}} - \Gamma_2\cdot\boldsymbol{\alpha}_{n+1}\right)d^2\bar{\varepsilon} = \boldsymbol{\Omega}d^2\bar{\varepsilon} \tag{44}$$

Substituting equations (42) and (44) into the equation (39) after taking derivative the increment of consistency parameter becomes

$$d^2\bar{\varepsilon} = \frac{\mathbf{m}_{n+\beta}\bar{\mathbf{C}}d\boldsymbol{\varepsilon}_{n+1}}{\mathbf{m}_{n+\beta}\bar{\mathbf{C}}\mathbf{m}_{n+\beta} - d\bar{\varepsilon}\mathbf{m}_{n+\beta}(\mathbf{M}_{n+\beta}\cdot\boldsymbol{\Omega}) + \mathbf{m}_{n+\beta}\boldsymbol{\Omega} + d\bar{\sigma}_{iso}/d\bar{\varepsilon}} \tag{45}$$

Therefore the consistent tangent modulus is calculated by substituting the equation (45) into equation (42).

$$\bar{\mathbf{C}}^{ep} = d\frac{d\boldsymbol{\sigma}_{n+1}}{d\boldsymbol{\varepsilon}_{n+1}} = \left[\bar{\mathbf{C}} - \frac{\bar{\mathbf{C}}\mathbf{m}_{n+\beta}\otimes\bar{\mathbf{C}}\mathbf{m}_{n+\beta} - d\bar{\varepsilon}(\bar{\mathbf{C}}\mathbf{M}_{n+\beta})\boldsymbol{\Omega}\otimes\bar{\mathbf{C}}\mathbf{m}_{n+\beta}}{\mathbf{m}_{n+\beta}\bar{\mathbf{C}}\mathbf{m}_{n+\beta} - d\bar{\varepsilon}\mathbf{m}_{n+\beta}\bar{\mathbf{C}}(\mathbf{M}_{n+\beta}\boldsymbol{\Omega}) + \mathbf{m}_{n+\beta}\boldsymbol{\Omega} + d\bar{\sigma}_{iso}/d\bar{\varepsilon}}\right] \tag{46}$$

To complete the consistency tangent modulus, the derivative $\mathbf{M}_{n+\beta}$ should be calculated and the results are expressed in Appendix.

In this paper, based on the numerical formulations developed above, the constitutive law for the anisotropic Drucker-Prager criterion is implemented into the commercial finite element code ABAQUS using the implicit user subroutine UMAT [21]. Note that all stresses, strains, and state variables are defined in the local material axes for anisotropic materials. These local material axes form a basis system in which stress and strain components are stored. This represents a co-rotational coordinate system in which the basis system rotates with the material. At the beginning of stress update routine in UMAT, the given stress and strain are automatically rotated values in the co-rotated coordinate system but the other state variables such as back stress and plastic strain should be rotated to account for the evolution of the material directions. The rotation effect is treated using the rotation matrix which is decomposed from the deformation gradient tensor ($\mathbf{R} = \mathbf{F}\mathbf{U}^{-1}$).

Verification

In this part, the developed constitutive equations are validated using the measured material properties. The initial yield stress and hardening data for Ti-4Al-0.2O_2 by Lee and Backofen [22] are utilized and the values are summarized in Table 1. From the table, the Ti-4Al-0.2O_2 has anisotropic and asymmetric properties as well. From the tensile and compressive data the material parameters have been calculated using equation (12) for yield criterion and equation (21) for hardening evolution law. Here, since the shear data is not available, only the results of principal directions are considered. In Table 2, calculated material parameters are listed. Figure 4 shows the calculated yield criterions which well represent the anisotropy and asymmetry and their evolution in the material directions x and y. The different hardening rates in the x- and y-directions are illustrated in Figure 5. From this

Table 1. Measured yield strength with respect to plastic strain [22]

Plastic strain	σ_x (MPa) (tensile, x-direction)	σ_x (MPa) (compressive, x-direction)	σ_y (MPa) (tensile y-direction)	σ_y (MPa) (compressive, y-direction)
0.000	644.7	513.7	689.5	455.1
0.002	658.5	589.5	692.9	530.9
0.010	706.7	751.6	713.6	727.4
0.040	772.2	861.9	751.6	879.1

Table 2. Material parameters for the yield surface and hardening

Parameters	Values
p	1.119
β_{22}	1.027
β_{33}	1.0
q	−1.023
α_0	34.891 (MPa)
g_{11}	8051.3 (MPa)
g_{22}	2745.2 (MPa)
g_{33}	0
h_{11}	56.54
h_{22}	31.78
h_{33}	0

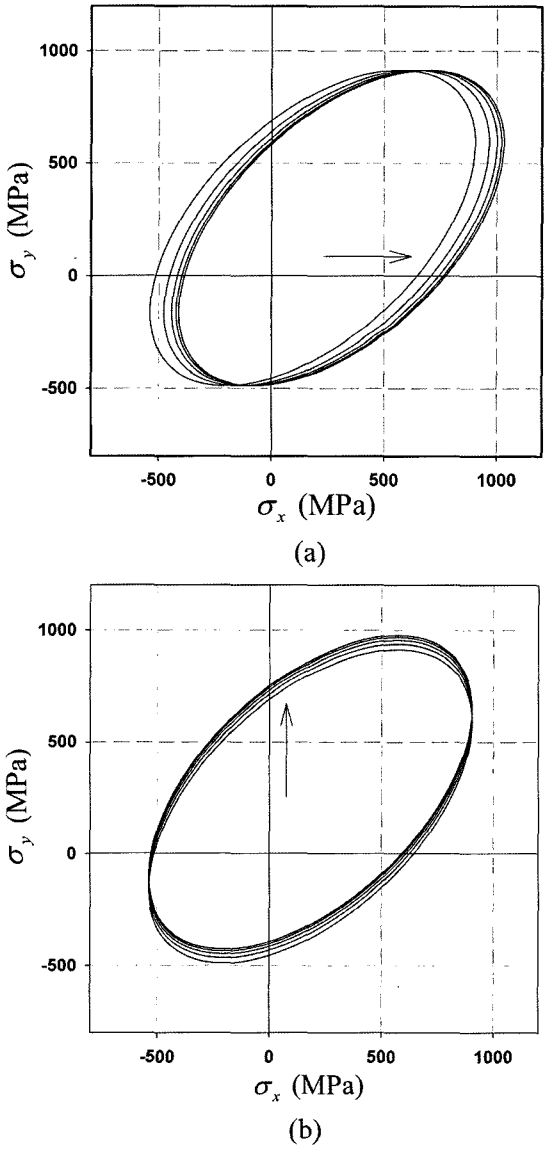

Figure 4. Calculated yield surfaces and their evolution in the material directions: (a) x and (b) y.

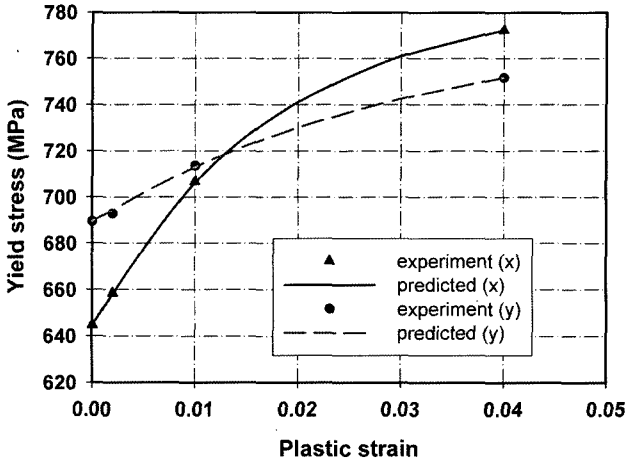

Figure 5. Hardening curves in the x and y directions.

example, the developed constitutive equations would be adequate for the highly anisotropic and asymmetric materials with the initial yield criterion as well as subsequent hardening data.

Summary

In order to represent the material behavior of highly anisotropic and asymmetric materials, a constitutive model was developed and its numerical implementation procedures were presented based on the elasto-plasticity theory. The Drucker-Prager yield criterion was modified to consider both the anisotropic and asymmetric properties by adding anisotropic parameters and initial translation of yield surface. Also, a kinematic hardening law was introduced to describe anisotropic hardening behavior by modifying the Chaboche type back-stress evolution rule. In addition to the constitutive equation, stress integration algorithm based on the elasto-plasticity was presented based on the incremental deformation theory. The implementation procedure for the developed theory and algorithms was presented for the implicit finite element method with consistent tangent modulus and the numerical example was illustrated with measured material data of reported article.

Acknowledgement

The authors of this paper would like to thank the Korea Science and Engineering Foundation (KOSEF) for sponsoring this research through the SRC/ERC Program of MOST/ KOSEF (R11-2005-065).

References

1. W. Lee, J. H. Kim, H.-J. Shin, K. Chung, T. J. Kang, and J. R. Youn, *Fibers and Polymers*, **4**, 77 (2003).

2. M. R. Piggot and B. Harris, *J. Mater. Sci.*, **15**, 2523 (1980).
3. N. L. Hancox, *J. Mater. Sci.*, **10**, 234 (1975).
4. M. G. Lee, K. Chung, C. J. Lee, J. H. Park, J. Kim, T. J. Kang, and J. R. Youn, *Composites Science and Technology*, **61**, 2491 (2001).
5. A. F. Saleeb, T. E. Wilt, N. R. Al-Zoubi, and A. S. Gendy, *Composites Part B*, **34**, 21 (2003).
6. B. D. Agarwal and L. J. Broutman, "Analysis and Performance of Fiber Composites", John Wiley & Sons, NY, 1980.
7. A. S. Khan and S. Huang, "Continuum Theory of Plasticity", John Wiley & Sons, NY, 1995.
8. R. Hill, "The Mathematical Theory of Plasticity", Oxford University Press, NY, 1956.
9. F. Barlat, D. J. Lege, and J. C. Brem, *International Journal of Plasticity*, **7**, 693 (1991).
10. F. Barlat, J. C. Brem, J. W. Yoon, K. Chung, R. E. Dick, S.-H. Choi, F. Pourboghrat, E. Chu, and D. J. Lege, *International Journal of Plasticity*, **19**, 1297 (2003).
11. A. R. Leewood, J. F. Doyle, and C. T. Sun, *Comput. Struct.*, **25**, 749 (1987).
12. L. P. Isupov and Yu. N. Rabotnov, *Izv. AN SSSR MTT*, **1**, 121 (1985).
13. B. S. Sarbayev, *Computational Materials Science*, **6**, 211 (1991).
14. M. G. Lee, D. Kim, K. Chung, J. R. Youn, and T. J. Kang, *Polymer and Polymer Composites*, **12**, 225 (2004).
15. J. L. Chaboche, *International Journal of Plasticity*, **2**, 149 (1986).
16. R. M. Jones, "Mechanics of Composite Materials", McGraw-Hill, NY, 1975.
17. K. Chung, M.-G. Lee, D. Kim, C. Kim, M. L. Wenner, and F. Barlat, *International Journal of Plasticity*, **21**, 861 (2005).
18. S. W. Tsai and E. M. Wu, *J. Comp. Mater.*, **5**, 58 (1971).
19. J. W. Yoon, D. Y. Yang, and K. Chung, *Computer Methods in Applied Mechanics and Engineering*, **174**, 23 (1999).
20. J. C. Simo and T. J. R. Hughes, "Computational Inelasticity", Springer-Verlag, N.Y., U.S.A., 1997.
21. Hibbitt, Karlsson and Sorensen, "ABAQUS User's Manual", Version 6.2.6., 2001.
22. D. Lee and W. A. Backofen, *Trans. Metall. Soc. AIME*, 236 (1966).

Appendix

Yield surface normal $\mathbf{m}(\equiv \partial\bar{\sigma}/\partial\boldsymbol{\sigma})$ and its derivative $\partial\mathbf{m}/\partial\boldsymbol{\sigma}$ $(\equiv \partial^2\bar{\sigma}/\partial\boldsymbol{\sigma}\partial\boldsymbol{\sigma})$ for the modified Drucker-Prager yield surface are defined as following.

A. $\partial\bar{\sigma}/\partial\boldsymbol{\sigma}$

$$\frac{\partial\bar{\sigma}}{\partial\sigma_x} = \frac{1}{2}p\frac{2\sigma_x-\beta_{22}(\sigma_y-\alpha_0)}{\Delta} - q$$

$$\frac{\partial\bar{\sigma}}{\partial\sigma_y} = \frac{1}{2}p\frac{(-\beta_{22}\sigma_x+2\beta_{22}^2(\sigma_y-\alpha_0))}{\Delta} - q\beta_{22}$$

$$\frac{\partial\bar{\sigma}}{\partial\sigma_{xy}} = 3p\frac{\beta_{33}^2\sigma_{xy}}{\Delta}$$

where

$$\Delta = \sqrt{\sigma_x^2-\beta_{22}\sigma_x(\sigma_y-\alpha_0)+\beta_{22}^2(\sigma_y-\alpha_0)^2+3\beta_{33}^2\sigma_{xy}^2}$$

B. $\partial^2\bar{\sigma}/\partial\boldsymbol{\sigma}\partial\boldsymbol{\sigma}$

$$\frac{\partial^2\bar{\sigma}}{\partial\sigma_x^2} = \frac{3}{4}p(\beta_{22}^2(\sigma_y-\alpha_0)^2+4\beta_{33}^2\sigma_{xy}^2)/\Delta^3$$

$$\frac{\partial^2\bar{\sigma}}{\partial\sigma_y^2} = \frac{3}{4}p\beta_{22}^2(\sigma_x^2+4\beta_{33}^2\sigma_{xy}^2)/\Delta^3$$

$$\frac{\partial^2\bar{\sigma}}{\partial\sigma_{xy}^2} = 3p\beta_{33}^2(\sigma_x^2-\beta_{22}(\sigma_y-\alpha_0)(\sigma_x-\beta_{22}(\sigma_y-\alpha_0)))/\Delta^3$$

$$\frac{\partial^2\bar{\sigma}}{\partial\sigma_x\partial\sigma_y} = -\frac{3}{4}p\beta_{22}^2(\beta_{22}\sigma_x(\sigma_y-\alpha_0)+2\beta_{33}^2\sigma_{xy}^2)/\Delta^3$$

$$\frac{\partial^2\bar{\sigma}}{\partial\sigma_x\partial\sigma_y} = \frac{\partial^2\bar{\sigma}}{\partial\sigma_y\partial\sigma_x}$$

$$\frac{\partial^2\bar{\sigma}}{\partial\sigma_x\partial\sigma_{xy}} = -\frac{3}{2}p(2\sigma_x-\beta_{22}(\sigma_y-\alpha_0))/\Delta^3$$

$$\frac{\partial^2\bar{\sigma}}{\partial\sigma_{xy}\partial\sigma_x} = \frac{\partial^2\bar{\sigma}}{\partial\sigma_x\partial\sigma_{xy}}$$

$$\frac{\partial^2\bar{\sigma}}{\partial\sigma_y\partial\sigma_{xy}} = \frac{3}{2}p\beta_{22}\beta_{33}^2\sigma_{xy}(\sigma_x-2\beta_{22}(\sigma_y-\alpha_0))/\Delta^3$$

$$\frac{\partial^2\bar{\sigma}}{\partial\sigma_{xy}\partial\sigma_y} = \frac{\partial^2\bar{\sigma}}{\partial\sigma_y\partial\sigma_{xy}}$$